AIP Advances

2D large-scale EWOD devices with honeycomb electrodes for multiplexed multidirectional driving of micro-droplets

Cite as: AIP Advances **10**, 055227 (2020); https://doi.org/10.1063/5.0008071
Submitted: 21 March 2020 . Accepted: 30 April 2020 . Published Online: 26 May 2020

Kaidi Zhang, Wei Wang, Chunqiao Li, Antoine Riaud, and Jia Zhou

2D large-scale EWOD devices with honeycomb electrodes for multiplexed multidirectional driving of micro-droplets

Cite as: AIP Advances 10, 055227 (2020); doi: 10.1063/5.0008071
Submitted: 21 March 2020 • Accepted: 30 April 2020 •
Published Online: 26 May 2020

Kaidi Zhang, Wei Wang, Chunqiao Li, Antoine Riaud, and Jia Zhou[a)]

AFFILIATIONS

ASIC and System State Key Lab, School of Microelectronics, Fudan University, Shanghai 200433, China

[a)]Author to whom correspondence should be addressed: jia.zhou@fudan.edu.cn

ABSTRACT

Chemical and biological applications could strongly benefit from large-scale droplet manipulation of electrowetting-on-dielectric (EWOD). However, the large number of driving electrodes of EWOD chips has been one of the most significant obstacles for these applications. This paper unveils a compact printed circuit board based EWOD chip with a hexagonal electrode array, which uses only seven signals to control an unlimited number of driving electrodes (169 in this paper). Simulation and experimental results illustrate the device's ability to transport multiple droplets synchronously with a reconfigurable driving route and a velocity of up to 10.0 mm/s, which is beneficial for complex or high-throughput EWOD applications.

Electrowetting-on-dielectric (EWOD) devices have been proven to be useful for many chemical and biological applications.[1–5] In these devices, the manipulation of droplets, such as generation, transportation, mixing, heating, detection, and so on, happens on a pattern of electrodes externally controlled by a series of pins. Combining these operations demands large-scale two-dimensional (2D) EWOD chips to carry out complex sample (pre-)treatment. Large-scale 2D EWOD chips are also a prerequisite for process parallelization and high throughput. For example, an on-chip PCR (polymerase chain reaction) process[6–8] requires multiple droplet cycles through different temperature regions. Cell culture[9–11] calls for a set of reagents and wastes to be moved in or out of the cell-culture area. Drug screening[12,13] requires parallel sample manipulation to improve the screening speed. With one pin per electrode, conventional EWOD devices are practically limited by the huge number of pins needed for high throughput applications.

Kim and co-workers were the first to propose an EWOD device driven by N(row) + M(column) control pins instead of N × M ones.[14] The chip was made of two plates with long strip electrodes laid at right angles with a gap. Electrowetting driving of droplets existed only at the intersection of the upper and lower electrodes. However, such a scheme might lead to serious electrode interference and had limited ability to drive more than two droplets on the chip or at the same time. Hadwen *et al.* developed a programmable large-scale AM-EWOD (active matrix electrowetting on dielectric) chip based on the technology of a thin film transistor (TFT) with a 64 × 64 electrode array.[15] However, such an integrated product is highly customized, resulting in prohibitive costs.

An effective solution to this problem is to use multiplexing, in which a set of electrodes is connected to the same electrical control line (pin). Multiplexing is particularly suitable for parallel applications with high throughput, such as PCR, where the same sequence of multiple droplet operation should be executed simultaneously.

This paper unveils a proof-of-concept of multiplexing on a large-scale electrode array. A compact hexagonal electrode array was designed with seven pins controlling 169 electrodes. Theoretically, the number of electrodes can be extended infinitely with the same number of pins. Its ability to drive multiple droplets synchronously is verified by simulation. The device was manufactured based on a printed circuit board (PCB) substrate. Long-distance transportation of a single droplet and a reconfigurable route of multiple droplets have been demonstrated. The velocity of moving droplets was also measured.

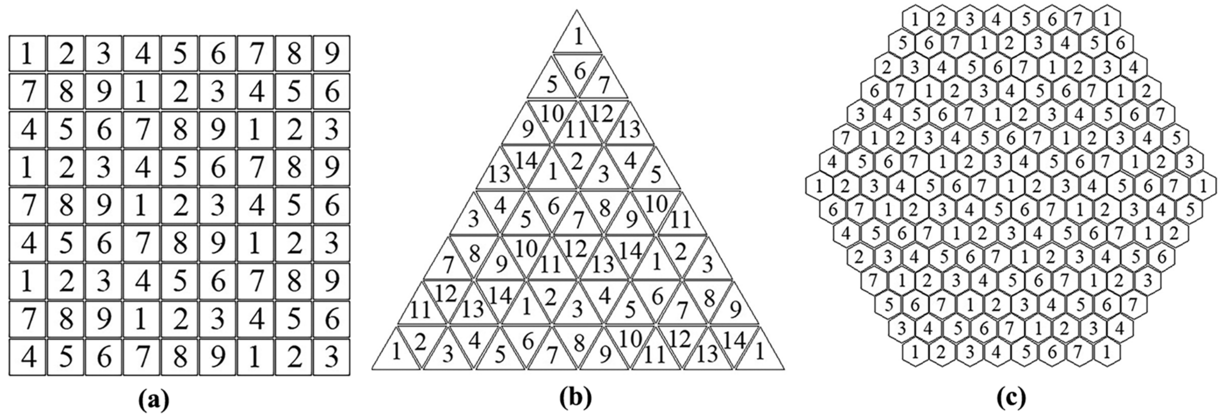

FIG. 1. Schematic of the coded 2D array formed by a (a) square, (b) triangle, and (c) hexagon.

To design a multiplexed large-scale 2D array, three rules should be followed in order to drive the droplets correctly:

1. Two adjacent electrodes should be activated by different pins so that the droplet can be driven from one electrode to another.
2. For a given electrode, the pins of all the surrounding electrodes should be different from each other so that the droplet can be driven in a unique direction. The surrounding should include all the electrodes sharing a vertex with this electrode.
3. Combining rules 1 and 2, we find that in order to form a large-scale array with the minimum number of pins, the multiplexing code of the electrodes should form a periodic pattern over the whole chip.

Generally, three basic shapes of electrodes can possibly be the elementary unit: equilateral triangle, square, and regular hexagon,[16,17] as shown in Fig. 1. Electrodes with the same code can be connected together.

Considering the neighboring electrodes (sharing the same vertices), the minimum number of pins is nine for a square array [Fig. 1(a)], 14 for a triangular array [Fig. 1(b)], and seven for a hexagonal array [Fig. 1(c)]. Therefore, a hexagonal array should be the best for a 2D EWOD structure with the least number of necessary control pins. Besides, the hexagonal array will increase the droplet transportation precision because the droplet has six directions to move.[18]

For a honeycomb array, each hexagon is adjacent with six neighboring hexagons. Therefore, the minimum number of necessary pins is seven to meet rules 1 and 2. In addition, seven pins are enough to fulfill the droplet manipulation on the whole array, according to rule 3.

It should be noted that the required number of electrical pins is independent of the number of electrodes, which can be theoretically infinite. For any regular hexagonal electrode, there is no electrode adjacent to it diagonally (all the neighbors share exactly one edge). Therefore, the motion of a droplet is completely symmetrical in all six directions, which makes the driving route very flexible. Since each neighbor electrode in the honeycomb array is controlled by a different pin, moving the droplet in any direction is as simple as controlling a 1D EWOD device, without the necessity to control both row and column pins. The structure and operation mode of such a 2D honeycomb array EWOD device are greatly simplified compared

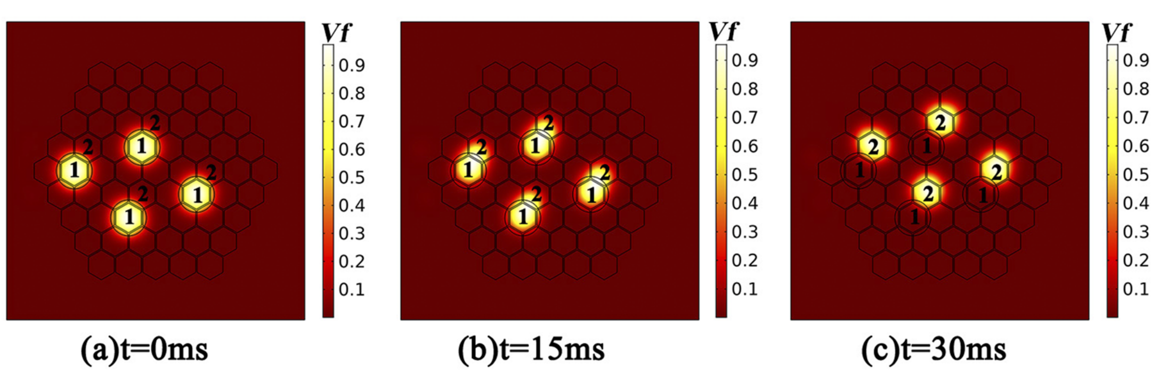

FIG. 2. Simulation of distributions of voltage and the liquid volume fraction in the process of multiple droplet transportation.

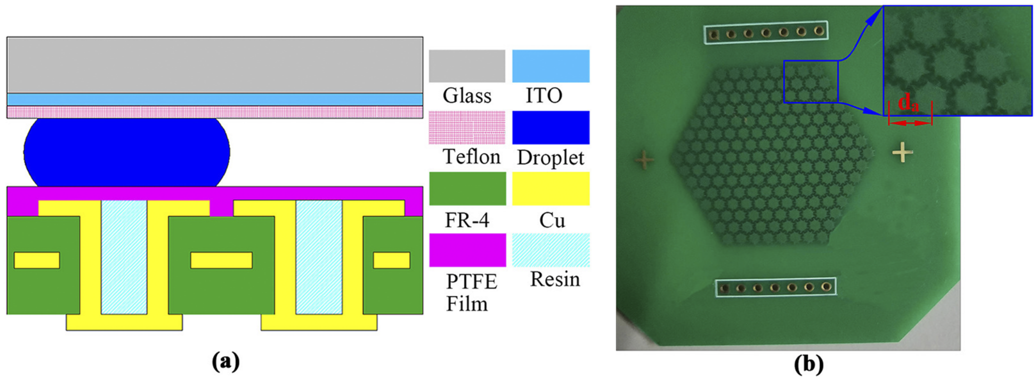

FIG. 3. 2D PCB-based hexagonal EWOD device: the (a) schematic and (b) image of the prototype.

with the N × M electrode 2D array. In addition, the device can transport multiple droplets at the same time as long as the droplets are on the electrode with the same code.

In order to verify the design of the hexagonal electrode array, Comsol Multiphysics® is used to simulate the process of the transportation of droplets numerically.

A "two-phase flow, level set" model enables 3D interface tracking and CA (contact angle) specification. The electrowetting effect is set using wetted-wall boundary conditions. During the simulation, the active electrodes are polarized with 140 V DC, while those on the others are grounded to 0 V.

The movement of droplets under the voltage shift is illustrated in Figs. 2(a)–2(c). The four black circles represent the original places of the four droplets, which are best demonstrated in Fig. 2(c). V_f is the volume fraction of the liquid. Numbers "1" and "2" are manually drawn to indicate the original and destination electrodes. Between 0 ms and 15 ms, both pins "1" and "2" are "on" to elongate the droplets, which stretch toward the electrodes connected to "2." When pin "1" is released, the droplets are dragged to the electrodes marked "2" (15–30 ms). All the four droplets behave synchronously under the voltage shift.

For reliable EWOD manipulation, the droplet should be slightly larger than an electrode. However, droplets with a diameter exceeding 1.44 times the diagonal length of the hexagonal electrode tend to split upon actuation. This is because the droplet will spread over an area larger than two electrodes and will eventually be in contact with two "on" electrodes at the same time. Therefore, it might be stretched in two opposite directions and split into two.

Figure 3 illustrates the design and prototype of the device. As shown in Fig. 3(a), the EWOD bottom plate is a three-layer PCB (printed circuit board) with the conductive resin filling the holes to make the surface flat.

Hydrophobic thin films like ETFE[19] or PTFE[20] can be used as the dielectric and hydrophobic layer on the PCB. The top plate is made of ITO glass with Teflon® AF as the hydrophobic layer. The gap between the electrodes is 200 μm. The pitch of the electrodes is 2 mm, as shown in Fig. 3(b). The border of each hexagon is designed like gears to minimize the gap between the electrodes. The vias are connected to each other by tracks in the middle and bottom layers to form the structure as shown in Fig. 1(c).

The assembly process is as follows:

1. Clean the PCB surface and dry it.
2. Cut the PTFE film, and stick it on the PCB after stretching.
3. Apply a small amount of 5 cSt silicone oil to cover the PTFE surface evenly.
4. Position the top plate with a silicon spacer.

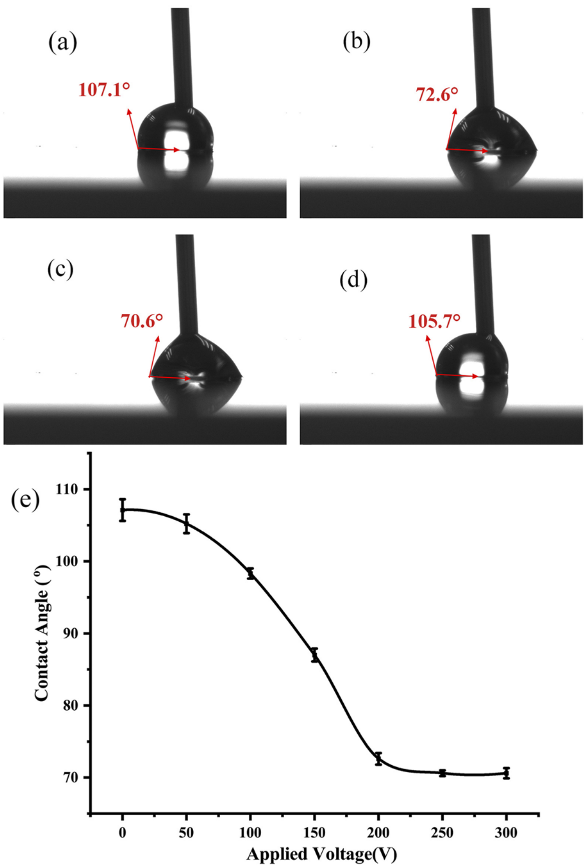

FIG. 4. CA test of the PTFE film: (a) 107.1° at 0 V, (b) 72.6° at 200 V, (c) 70.6° at 300 V, (d) 105.7° after powering off, and (e) CA vs applied voltage.

De-ionized (DI) water droplets were used in the experiments. The CA of the droplet was measured over a range of positive voltage supply. Here, the electrode on the PCB is grounded, and a probe connected to a positive high voltage is in contact with the droplet. The reverse situation might result in different CAs as observed with a nano-scale droplet[21] or polar materials,[22] but the curve remains approximately symmetrical in most cases. The voltage was increased incrementally by 50 V from 0 V to 400 V, and the CAs are measured and recorded by a drop shape analyzer (DSA30, KRÜSS, Germany). The reverted CA was also measured after turning off the electrical excitation.

AC signals were used for manipulating the droplets in order (i) to reduce the CA hysteresis[23] and (ii) increase reliability by avoiding the build-up of charges on the insulators.[24] The driving signals are provided by a signal generator (FG503, MOTECH, Taiwan, China) and boosted by a high-voltage amplifier (ATA-2082, ATek, China). The frequency of the applied voltage is set to 1 kHz, and the amplitude could vary from 0 to 800 V_{pp} or 282 V_{rms}. The electrodes are controlled by self-made cellphone-based software (app) with a simplified controlling circuit. The droplet manipulation routine can be pre-defined or controlled in real-time. Their movement is recorded by a CCD camera (TK-C9201EC, JVC, Japan). In order to increase the contrast between the droplet and the background, a small amount of ink is added to the deionized water.

During single droplet experiments, a long-distance round-trip is set to observe (i) the conditions for droplet motion and (ii) the displacement of a droplet on the device. During multiple droplet experiments, seven droplets are placed on the electrodes with the same code. They are manipulated synchronously with a flexible routine.

The average droplet velocity is measured by recording the droplet displacement during a hexagonal circulation routine. At constant volume, the size of the droplet is adjusted by changing the gap between the top plate and the PCB bottom plate using silicon spacers. The applied voltage varies from 0 to 282 V_{rms}. During the motion of droplets, the destination electrode would be "on" for a time period t_s to pull the droplet from the original one, while the latter is still "on" for $t_s/2$ and turned off afterward. The threshold value of t_s, t_{th}, is recorded when the motion of the droplet could not catch up with the voltage shift. The maximum velocity of the droplet v_{max} can be calculated as d_s/t_{th}.

The initial CA is about 107.1° after surface silicone oil treatment, as shown in Fig. 4(a). When the voltage increases up to 200 V, the CA decreases by about 40° until the CA saturates near 70°, as shown in Figs. 4(b) and 4(c). We did not observe any breakdown even for voltages as high as 300 V. After powering off, the CA reverts to 105.7° [Fig. 4(d)], which demonstrates the feasibility of the EWOD device. Figure 4(e) shows the relationship between the CA and the applied voltage with error bars.

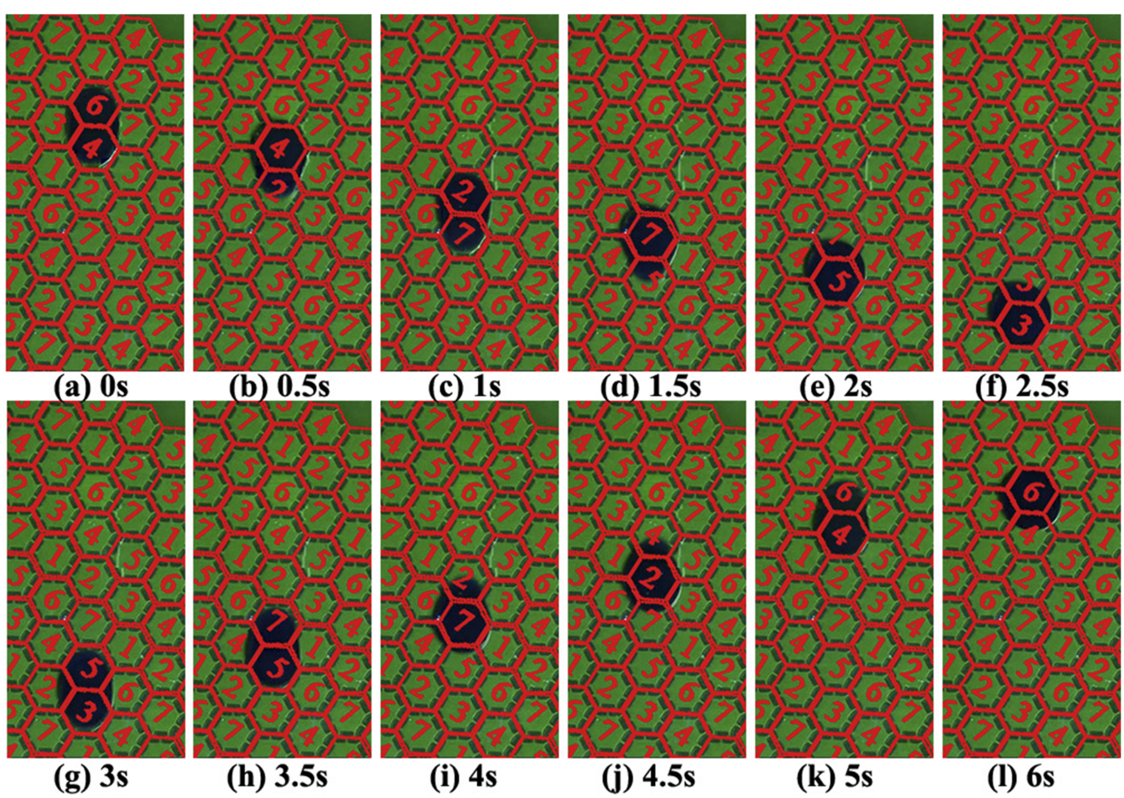

FIG. 5. [(a)–(l)] motion of a single droplet during a long-distance round-trip (the coding map of the electrode is superimposed on the photographs for clarity).

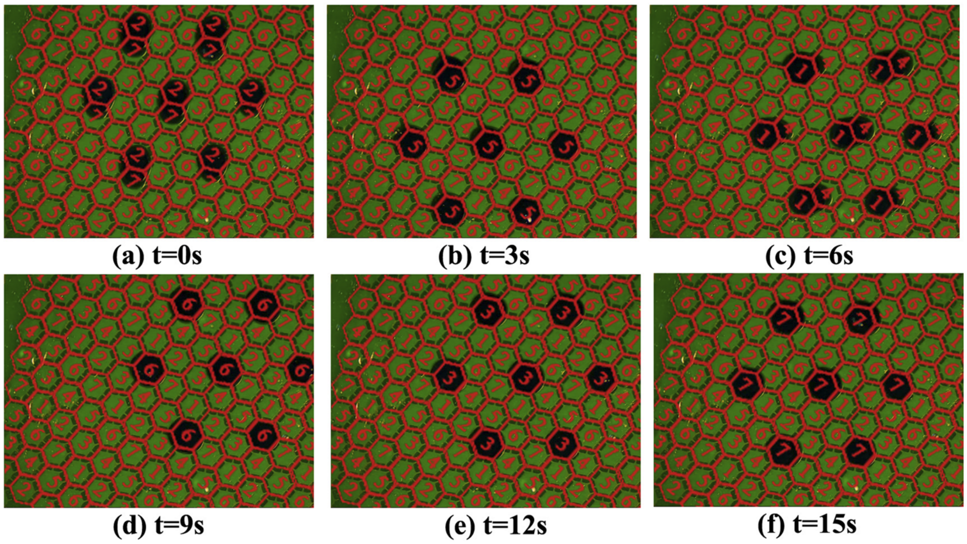

FIG. 6. [(a)–(f)] synchronized motion of multiple droplets (the coding map of the electrode is superimposed on the photographs for clarity).

Figures 5(a)–5(l) (supplementary material video S1) capture the long-distance round-trip of a single droplet with the routine of 6-4-2-7-5-3-5-7-2-4-6. The coding map of the electrode is superimposed on the photographs for clarity. It can be seen that the droplet accomplishes a straight trip back and forth several times. t_s is 500 ms, and the voltage is 150 V_{rms} with a 300 μm spacer.

Figures 6(a)–6(f) (supplementary material video S2) capture the synchronized transportation of seven droplets. The routine is controlled manually as "2-7-5-1-4-6-3-7." The parameters in this experiment are the same as that for the single droplet test. Thanks to its 6-fold symmetry, the droplets can move flexibly in any direction from any position. With a large enough surface area, such a device can drive an unlimited number of droplets theoretically.

It should be noted that several inlets and outlets can be integrated to the hexagon array so that the droplets can be moved from any inlet to any outlet to meet actual biological protocols.

The routine of the velocity test is set to "6-3-7-5-3-4-5-1-4-6-1-7-6." Figures 7(a)–7(f) (supplementary material video S3) show the droplet motion under 212 V_{rms} driving voltage with a t_{th} of 500 ms and a spacer of 500 μm. This indicates a maximum velocity v_{max} of 4 mm/s.

The relationship between velocity and applied voltage with different gap heights between the two plates is shown in Fig. 7(g). The maximum velocity increases with the gap height and the applied voltage, which agrees with theoretical studies.[25–28] When 145 V_{rms} is applied with a spacing of 500 μm, the droplet speed is limited to 1.1 mm/s. When the driving voltage reaches 282 V_{rms}, v_{max} increases to 10.0 mm/s, which is a little faster than previous studies on PCB-EWOD.[20]

However, when the spacing reaches 800 μm, v_{max} starts to behave in a parabolic trend rather than in the linear trend observed for smaller gaps. Remarkably, the displacement speed at low voltage becomes lower than for any other gap height. We tentatively attribute this trend to the droplet size; indeed, at 800 μm gap height,

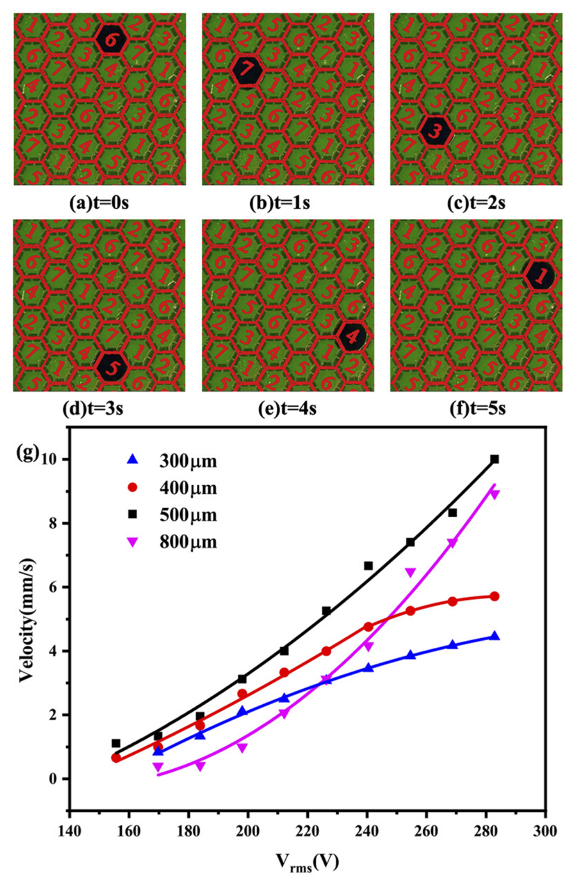

FIG. 7. Velocity of a droplet: [(a)–(f)] images of droplet circulation and (g) v_{max} vs applied voltage with different spacings.

the droplet becomes so small that it hardly reaches the nearby electrodes, thereby delaying the droplet motion (0.4 mm/s at 170 V_{rms}). At high voltage, the droplet may be more spread-out, thereby allowing the droplet to reach a larger fraction of the next electrode and accelerating the droplet motion (8.9 mm/s at 282 V_{rms}).

As a summary, in order to provide a simpler and more flexible multi-droplet manipulation method, we propose a 2D EWOD array with a hexagonal electrode structure with only seven pins to control an unlimited number of electrodes (169 in this device). The chip is fabricated in a fast and low-cost manner by directly making a hexagonal array on a PCB and adding a PTFE hydrophobic film infused with silicon oil. After optimization (282 V_{rms} driving voltage and 500 μm gap height), this structure allows the droplet speed to reach up to 10.0 mm/s. We then demonstrate the simultaneous transportation of multiple droplets over an arbitrary path on a theoretically unbounded hexagonal electrode array.

This research promises to simplify the droplet transportation in complex and/or high-throughput biochemical systems.

The process of Figs. 5–7 can be found in the supplementary material: Video S1, Video S2, and Video S3.

AUTHORS' CONTRIBUTIONS

K.Z. and W.W. contributed equally to this work.

This work was supported by the National Natural Science Foundation of China under Grant No. 61874033, the Natural Science Foundation of Shanghai Municipal Government under Grant No. 18ZR1402600, and the State Key Lab of ASIC and System, Fudan University, under Grant No. 2018MS003.

DATA AVAILABILITY

The data that support the findings of this study are available within the article and its supplementary material.

REFERENCES

[1]M. G. Pollack, V. K. Pamula, V. Srinivasan, and A. E. Eckhardt, "Applications of electrowetting-based digital microfluidics in clinical diagnostics," Expert Rev. Mol. Diagn. **11**, 393–407 (2011).

[2]E. Samiei, M. Tabrizian, and M. Hoorfar, "A review of digital microfluidics as portable platforms for lab-on a-chip applications," Lab Chip **16**, 2376–2396 (2016).

[3]G. Lu, D. Lin, and X. Wang, "Progress of electrowetting applications in micro-nano energy conversion and utilization systems," Chin. Sci. Bull. **62**, 799–811 (2016).

[4]Z. Zeng, K. Zhang, W. Wang, W. Xu, and J. Zhou, "Portable electrowetting digital microfluidics analysis platform for chemiluminescence sensing," IEEE Sensors J. **16**, 4531–4536 (2016).

[5]Y. Yu, J. Chen, J. Li, S. Yang, S.-K. Fan, and J. Zhou, "Microfabrication of a digital microfluidic platform integrated with an on-chip electrochemical cell," J. Micromech. Microeng. **23**, 095025 (2013).

[6]J. Akagi, F. Zhu, C. J. Hall, K. E. Crosier, P. S. Crosier, and D. Wlodkowic, "Integrated chip-based physiometer for automated fish embryo toxicity biotests in pharmaceutical screening and ecotoxicology," Cytometry, Part A **85**, 537–547 (2014).

[7]Z. Hua, J. L. Rouse, A. E. Eckhardt, V. Srinivasan, V. K. Pamula, W. A. Schell, J. L. Benton, T. G. Mitchell, and M. G. Pollack, "Multiplexed real-time polymerase chain reaction on a digital microfluidic platform," Anal. Chem. **82**, 2310–2316 (2010).

[8]C. D. Ahrberg, A. Manz, and B. G. Chung, "Polymerase chain reaction in microfluidic devices," Lab Chip **16**, 3866–3884 (2016).

[9]I. A. Eydelnant, U. Uddayasankar, B. Li, M. W. Liao, and A. R. Wheeler, "Virtual microwells for digital microfluidic reagent dispensing and cell culture," Lab Chip **12**, 750–757 (2012).

[10]S. M. George and H. Moon, "Digital microfluidic three-dimensional cell culture and chemical screening platform using alginate hydrogels," Biomicrofluidics **9**, 024116 (2015).

[11]I. Barbulovic-Nad, S. H. Au, and A. R. Wheeler, "A microfluidic platform for complete mammalian cell culture," Lab Chip **10**, 1536–1542 (2010).

[12]F. Eduati, R. Utharala, D. Madhavan, U. P. Neumann, T. Longerich, T. Cramer, J. Saez-Rodriguez, and C. A. Merten, "A microfluidics platform for combinatorial drug screening on cancer biopsies," Nat. Commun. **9**, 2434 (2018).

[13]A. Weltin, K. Slotwinski, J. Kieninger, I. Moser, G. Jobst, M. Wego, R. Ehret, and G. A. Urban, "Cell culture monitoring for drug screening and cancer research: A transparent, microfluidic, multi-sensor microsystem," Lab Chip **14**, 138–146 (2014).

[14]J. Gong and C. J. Kim, "Direct-referencing two-dimensional-array digital microfluidics using multi-layer printed circuit board," J. Microelectromech. Syst. **17**, 257–264 (2008).

[15]F. A. Shaik, G. Cathcart, S. Ihida, M. Lereau-Bernier, E. Leclerc, Y. Sakai, H. Toshiyoshi, and A. Tixier-Mita, "Thin-film-transistor array: An exploratory attempt for high throughput cell manipulation using electrowetting principle," J. Micromech. Microeng. **27**, 054001 (2017).

[16]F. Su and K. Chakrabarty, "Yield enhancement of reconfigurable microfluidics-based biochips using interstitial redundancy," ACM J. Emerging Technol. Comput. Syst. **2**, 104–128 (2006).

[17]O. Keszocze, R. Wille, and R. Drechsler, "Pin-aware routing and extensions," in *Exact Design of Digital Microfluidic Biochips* (Springer International Publishing, Cham, 2019), pp. 55–85.

[18]A. Dutta, R. Majumder, D. Dhal, and R. Pal, "Structural and behavioural facets of digital microfluidic biochips with hexagonal-electrode-based array," in 32nd International Conference on VLSI Design and 2019 18th International Conference on Embedded Systems (VLSID) (2019), pp. 239–244.

[19]M. Alistar and U. Gaudenz, "Opendrop: An integrated do-it-yourself platform for personal use of biochips," Bioengineering **4**, 45 (2017).

[20]S. Zulkepli, N. Hamid, and V. Shukla, "Droplet velocity measurement based on dielectric layer thickness variation using digital microfluidic devices," Biosensors **8**, 45 (2018).

[21]D. Bratko, C. D. Daub, K. Leung, and A. Luzar, "Effect of field direction on electrowetting in a nanopore," J. Am. Chem. Soc. **129**, 2504–2510 (2007).

[22]P. Zhao, Y. Li, X. Zeng, J. Zhou, Y. Huang, and R. Liu, "EWOD using P(VDF-TrFE)," in *4th IEEE International Conference on Nano/Micro Engineered and Molecular Systems* (IEEE, 2009), pp. 202–205.

[23]J. Gao, N. Mendel, R. Dey, D. Baratian, and F. Mugele, "Contact angle hysteresis and oil film lubrication in electrowetting with two immiscible liquids," Appl. Phys. Lett. **112**, 203703 (2018).

[24]R. B. Fair, "Digital microfluidics: Is a true lab-on-a-chip possible?," Microfluid. Nanofluid. **3**, 245–281 (2007).

[25]P. Day, A. Manz, and Y. Zhang, *Microdroplet Technology* (Springer, 2012).

[26]C. Y. Chen, E. F. Fabrizio, A. Nadim, and J. D. Sterling, "Electrowetting-based microfluidic devices: Design issues," Summer Bioengineering Conference, Key Biscayne, FL, 2003, available at https://www.researchgate.net/publication/238083533_ELECTROWETTING-BASED_MICROFLUIDIC_DEVICES_DESIGN_ISSUES.

[27]J. R. Choudhuri, D. Vanzo, P. A. Madden, M. Salanne, D. Bratko, and A. Luzar, "Dynamic response in nanoelectrowetting on a dielectric," ACS Nano **10**, 8536–8544 (2016).

[28]H. Li, M. Paneru, R. Sedev, and J. Ralston, "Dynamic electrowetting and dewetting of ionic liquids at a hydrophobic solid-liquid interface," Langmuir **29**, 2631–2639 (2013).